Dynamical effects of confinement on atomic valence photoionization in Mg@C_{60}

Himadri S. Chakraborty,[1] Mohamed E. Madjet,[2] Jan-M. Rost,[3] and Steven T. Manson[4]
[1]*Department of Chemistry and Physics, Northwest Missouri State University, Maryville, Missouri 64468, USA*
[2]*Freie Universität, Institut für Chemie (Kristallographie), Takustrasse 6, D-14195 Berlin, Germany*
[3]*Max-Planck-Institut für Physik Komplexer Systeme, Nöthnitzer Strasse 38, D-01187 Dresden, Germany*
[4]*Department Physics and Astronomy, Georgia State University, Atlanta, Georgia 30303, USA*
(Received 25 March 2008; published 15 July 2008)

We predict a huge dynamical boost from collective electron motion on the valence 3*s* photoionization of Mg in the Mg@C_{60} molecule. Calculations have been performed in a framework of time-dependent local density approximation that includes coupling between dipole-allowed final state channels. Our results qualitatively agree with the recent predictions of a semiclassical model, however, significantly differing in magnitude. In particular, a strong dependence on the nature of the caged atom is found which is at odds with the prediction of the semiclassical result.

DOI: 10.1103/PhysRevA.78.013201 PACS number(s): 61.48.−c, 33.80.Eh, 36.40.Cg

I. INTRODUCTION

After it was discovered that the fullerenes are semispherical hollow molecules of carbon, researchers speculated that atoms, molecules, or clusters can be coaxed to occupy the space inside the cage. The existence of such endohedral fullerenes is now well established by experiment [1–3]. In fact, over the past several years it has been possible to synthesize fullerene compounds doped with a variety of atomic materials [4]. In addition to the possibility of studying the dynamical effects of the dopant on the electronic motion of the cage, the extraordinary geometric stability of the cage offers a unique natural laboratory to assess the behavior of the endohedral dopant in confinement. And since the typical size of this confinement is nanometers, novel quantum effects are exhibited in the properties of these systems [5]. In addition, the alteration of well-known static and dynamical features of free atoms can be examined under conditions of endohedral confinement.

Since these fullerenes and their derivatives are highly stable nanometric forms of carbon, they fascinate researchers with many exciting potential applications, including the following. (a) Research has been ongoing to use endofullerenes and doped bucky onions as seed materials in solid state quantum computations, in which qubits can be encoded in either electronic [6,7] or nuclear [8] spins of the encapsulated atoms. (b) Recent experiments with Ar@C_{60} find evidence of encaged atoms significantly improving the superconducting ability of materials [9]. (c) A proposed biomedical application of endohedral materials is to shield radioactive tracers inside fullerene cages, and then inject the material into human blood to monitor blood flow. (d) The ability of fullerenes to sequester one or more metal atoms inside the cage has led to research efforts aimed at exploring their potential as contrast-enhancing agents for magnetic resonance imaging. Such applications put into perspective the importance of understanding the static and dynamic properties of these systems. In addition, the discovery of endofullerenes with trapped noble gases in extraterrestrial environments [10] in larger amounts than can be synthesized in the laboratory indicates the relevance of the results even for astrophysical applications.

Understanding the influence of the confining cage on the atom inside is, therefore, a matter of significant basic and applied interest. Photoionization investigations offer an excellent probe owing to the weak photon-electron coupling, along with the fact that the photon disappears after the interaction. Recent semiclassical studies [11,12] have suggested that the photoabsorption cross section of an atom confined in C_{60} is dramatically affected in the neighborhood of the plasmons which occur in the photoionization of the C_{60} shell. This phenomenon has been partially confirmed (at least qualitatively) in a recent *ab initio* fully quantum mechanical calculation on Ar@C_{60} [13] where a huge increase of the Ar 3*p* cross section at the plasmon peak was found, quantitatively within a factor of 2 of the semiclassical prediction. The predicted decrease of the cross section below the plasmon peak could not be tested since the Ar 3*p* ionization threshold is located approximately at the plasmon peak. Thus, to test this, it is of interest to investigate a confined atom with a lower ionization potential. In addition, another useful case is to test the semiclassical prediction that the increase of the photoionization cross section of the confined atom compared to the free atom is a function of energy only and independent of the specific atom.

To further our understanding, in this paper we report on a study of the valence photoionization of Mg@C_{60}. This system was chosen because the ionization threshold of Mg 3*s* is significantly lower than Ar 3*p*, along with the fact that it is known that there is no transfer of valence electrons to the cage in Mg@C_{60} [14]. This study reveals that the atom-cage dynamical coupling produces spectacular effects, far larger than those envisioned by simple models [11,12].

II. BRIEF THEORETICAL DETAILS

Density functional theory was used to describe the electronic structure of the C_{60} cage as in previous works that (i) explained the measured oscillations in the valence photoelectron intensities of neutral C_{60} [15] and (ii) agreed well with a recent experimental study of the surface plasmon as well as a new higher-energy plasmon resonance in the photoionization of C_{60} cations [17,18]. In the formulation for the C_{60} ground

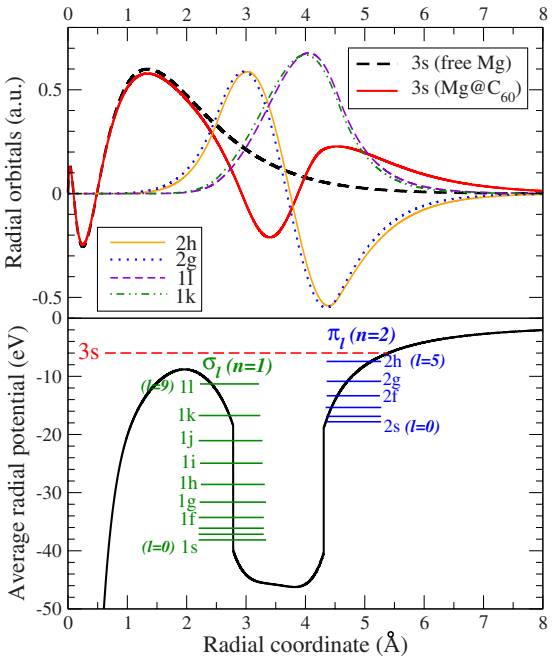

FIG. 1. (Color online) Bottom panel: The average radial LDA ground state potential. All C_{60} single-electron levels and the valence $3s$ levels of the confined Mg are shown. Top panel, free and confined Mg $3s$ radial wave functions. The radial wave functions of some pristine C_{60} levels are also displayed.

state, the four valence electrons $(2s^2 2p^2)$ of each carbon atom are rendered delocalized while the core C^{4+} ions (each consisting of a carbon nucleus plus two very tightly bound $1s$ electrons) are represented by a classical spherical jellium shell (with a radius $R=3.54$ Å and a thickness Δ), augmented by a constant potential V_0 [16]. We place Mg at the center of the sphere which is a good approximation, since the charge transfer interaction of the closed shell atom with the cage is weak [14]. The Kohn-Sham equations for the system of 252 electrons (12 from Mg and 240 delocalized electrons from the C_{60} cage) are then solved to obtain the ground state in the local density approximation (LDA). V_0 and Δ are determined by requiring charge neutrality and by producing the experimental value −7.54 eV of the binding energy of the highest occupied C_{60} orbital $(2h)$. The width Δ is found to be 1.5 Å. The ground state radial potential becomes orbital-specific owing to the correction to avoid self-interactions of electrons [19]. In Fig. 1 the average radial potential of the system is shown, along with the occupied single-electron energy levels. Note that the harmonic oscillator nomenclature is used for the cage levels, which are classified as $\sigma_l(n=1)$ and $\pi_l(n=2)$ where l denotes the orbital angular momentum with respect to the center. π wave functions have one radial node, while the σ wave functions are nodeless. Owing to the strong delocalization effect, the σ and π levels exhibit compact energy spacings and produce very nearly the same spectrum as the pristine (empty) C_{60}, indicating the stability of the cage's electronic structure. The atomic level, of which the valence $3s$ (−5.88 eV) is in this energy region, is also shown. The atomic wave function is partially hybridized, i.e., some mixing of the atomic wave functions occurs, as featured in an extra nodal structure in the vicinity of the cage in the radial $3s$ wave function (top panel, Fig. 1). Technically this wave function is of $5s$ character due to the two mixing-induced additional nodes. As a consequence of this hybridization, the $3s$ binding energy of confined Mg is reduced by about 24% compared to free Mg.

A time-dependent LDA (TDLDA) method [20,21] is employed to calculate the dynamical response of the system to the external dipole field. The perturbation z, the dipole interaction for linearly polarized light, induces a frequency-dependent complex change in the electron density arising from dynamical electron correlations. This can be written, using the LDA susceptibility χ_0, as

$$\delta\rho(\mathbf{r};\omega) = \int \chi_0(\mathbf{r},\mathbf{r}';\omega)\,\delta V(\mathbf{r}';\omega)d\mathbf{r}', \tag{1}$$

in which

$$\delta V(\mathbf{r}';\omega) = z + \int \frac{\delta\rho(\mathbf{r}';\omega)}{|\mathbf{r}-\mathbf{r}'|}d\mathbf{r}' + \left[\frac{\partial V_{\mathrm{xc}}}{\partial\rho}\right]_{\rho=\rho_0}\delta\rho(\mathbf{r};\omega), \tag{2}$$

where the second and third term on the right-hand side are, respectively, the induced change of the Coulomb and the exchange-correlation potentials. Obviously, in addition to containing the external perturbation z, δV also includes the dynamical field produced by important electron correlations. The photoionization cross section is then calculated as the sum of independent partial cross sections $\sigma_{nl\to kl'}$, corresponding to a dipole transition $nl\to kl'$:

$$\sigma_{\mathrm{PI}}(\omega) = \sum_{nl}\sigma_{nl\to kl'} \sim \sum_{n\ell} 2(2l+1)|\langle\phi_{kl'}|\delta V|\phi_{nl}\rangle|^2. \tag{3}$$

Clearly, replacing δV in Eq. (3) by z yields the LDA cross section that entirely omits the correlation. A more detailed description of the methodology used in the present calculations is presented elsewhere [22].

III. RESULTS AND DISCUSSIONS

Our results for the photoionization cross section of the $3s$ subshell of $Mg@C_{60}$ are shown in Fig. 2 along with the result for free Mg. The outstanding feature of these results is the huge increase in the cross section engendered by the confinement. This is similar to what was seen for $Ar@C_{60}$ $3p$ photoionization in comparison to free Ar $3p$ [13], with one important proviso. For the Ar case, the confinement increased the cross section by more than an order of magnitude, in the vicinity of the C_{60} plasmon, while for Mg the increase is almost three orders of magnitude; note that the cross section scale in Fig. 2 is logarithmic. In any case, Mg $3s$, much more than Ar $3p$, exhibits a huge increase in cross section in the vicinity of the dominant plasmon in pristine C_{60}, also shown in Fig. 2. Furthermore, the cross section increase stretches over a broad energy range, although away from the low-energy plasmon the magnitude increase is seen to be somewhat less, decreasing with energy-distance from the plasmon.

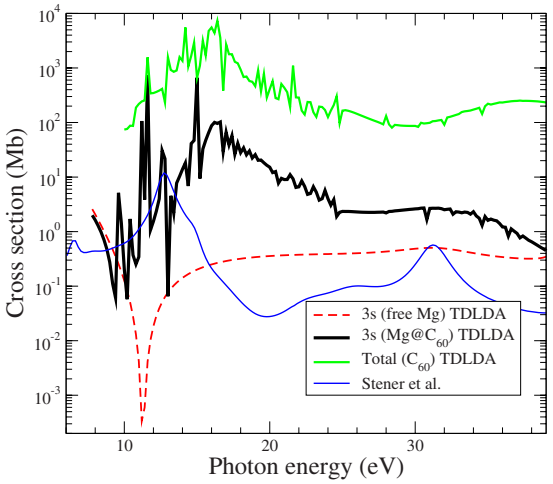

FIG. 2. (Color online) Free and confined Mg 3*s* photoionization cross sections calculated using the correlated TDLDA method, along with the total photoionization cross section of pristine C_{60} calculated in the same manner. Also shown is an earlier molecular calculation at the uncorrelated LDA level [23].

Shown also in Fig. 2 is the result of a molecular calculation of the photoionization of $Mg@C_{60}$ 3*s* [23] that treats the location of each C atom of the C_{60} correctly. However, the calculation was performed at essentially the single-particle (LDA) level and, thus the effects of the coupling to the plasmon maximum are entirely omitted. As a consequence, the resulting cross section is seen in Fig. 2 to be far too small overall, as compared to the present results. The cross section of Ref. [23] does, however, show the expected confinement-induced oscillations [15,25], indicating that the oscillations induced by the approximate jelliumlike potential are not artifacts. In any case, comparison of the two calculations emphasizes the importance of interchannel coupling between the photoionization channels of the confined atom with those of the confining shell, particularly in the neighborhood of a plasmon resonance in the shell.

In addition, the oscillator strength sum (integral) for the limited energy range from the ionization threshold up to 60 eV is 0.284 for free Mg 3*s* and 5.70 for $Mg@C_{60}$ 3*s*, an increase by more than a factor of 20 as a result of the confinement. Since the sum over only part of the confined 3*s* oscillator strength distribution is significantly greater than the sum rule [24,26] value of 2, the number of electrons in the 3*s* subshell, it is evident that the 3*s* subshell has been augmented significantly; the only possible source of added oscillator strength of this magnitude is the C_{60} shell of 240 delocalized electrons. The calculation confirms that the confinement-induced increase in cross section is due to the interchannel coupling of the 3*s* photoionization matrix elements with the dipole matrix elements of the shell electrons, similar to the case of confined Ar [13]. However, owing to the increased hybridization of the 3*s* wave function of confined Mg (see Fig. 1) as compared to the hybridization of confined Ar 3*p*, the interchannel coupling is rather larger in the Mg case, leading to the huge confinement-induced $Mg@C_{60}$ 3*s* cross section seen in Fig. 2.

Furthermore, the dramatic increase of the 3*s* cross section in going from free to confined Mg, owing to interchannel coupling, demonstrates that the confined cross section is almost completely driven by this interchannel coupling. As further evidence, it is clear from Fig. 2, that the prominent Cooper minimum in the free cross section at about 11 eV is completely obliterated in the confined case. This, along with the alteration of total oscillator strength, provides striking confirmation that the physics of the free cross section is quite different than the physics of the confined cross section, at least in the neighborhood of the giant plasmon resonance.

A recent semiclassical model has predicted the screening of an atom confined in a fullerene [11,12]. Semiclassically, for an atom enclosed by a dielectric shell in an external field the dynamical screening factor is connected to a power series in atomic polarizability [see Eq. (14) in Ref. [12]]. This result is exact, but the model is developed by only retaining the leading term (power zero) of the series by making the approximation that the atomic polarizability is negligible. This yields a dynamical screening curve independent to the central atom—a universal curve [Eq. (21) in Ref [12]]. The increase of the cross section in the present calculation in the neighborhood of the lower-energy plasmon excitation of C_{60} confirms, at least qualitatively, the prediction of this simple semiclassical model. This model also predicts a falloff of the cross section at lower energy, actually going to zero at zero energy. The $Mg@C_{60}$ 3*s* calculation does not go down to zero photon energy, but to 5.88 eV, the ionization threshold for $Mg@C_{60}$. This is low enough for the falloff to be observed in Fig. 2, where the confined 3*s* cross section is seen to drop rapidly with decreasing energy and actually lies below the free cross section below about 10 eV.

Moreover, the semiclassical model predicts a smaller, but still significant, enhancement of the photoionization cross section of an atom confined in C_{60} in the neighborhood of the higher-energy plasmon; this prediction is borne out by the calculation, as seen in Fig. 2, where the enhancement of the $Mg@C_{60}$ 3*s* cross section in the neighborhood of 35 eV is evident. Thus, qualitatively, the major predictions of the semiclassical model are all in agreement with *ab initio* quan-

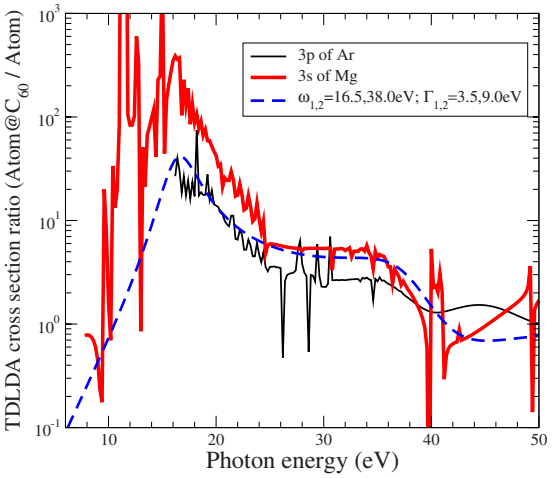

FIG. 3. (Color online) Ratio of the 3*s* photionization cross sections of $Mg@C_{60}$ and free Mg, the corresponding ratio for Ar 3*p* [13] and the predictions of the semiclassical model [11,12] using input parameters from the present calculation for consistency.

tum mechanical calculations. But what about quantitative accuracy?

To study this question the ratios of the confined versus free cross sections for Mg $3s$ and Ar $3p$ [13] are shown in Fig. 3, along with the dynamical screening factor predicted by the semiclassical model [12] using our calculated positions and widths for the C_{60} plasmons for consistency; note that the dynamical screening factor is the semiclassical analog of the cross section ratio. The outstanding feature of this comparison is that the semiclassical prediction is a single universal curve, while the calculated ratios differ at the maximum by more than an order of magnitude. Thus, the ratio is clearly quantitatively specific to the atomic species confined in the C_{60} so that a universal ratio cannot be correct. The quantitative agreement of the semiclassical universal curve with the $Ar@C_{60}$ $3p$ is not bad, generally better than a factor of 2, but for $Mg@C_{60}$, there is a quantitative discrepancy of about an order of magnitude in the vicinity of the giant plasmon resonance, as seen in Fig. 3.

IV. CONCLUSION

In summary then, a huge increase (three orders of magnitude) in the $3s$ photoionization cross section of $Mg@C_{60}$ as compared to free Mg, has been found. As was the case for confined Ar [13], this increase has been traced to the interchannel coupling of atomic photoionization channels with the photoionization channels of the confining shell, in the region of the giant plasmon resonance. In addition, the present work confirms the qualitative validity of a semiclassical model of the process [11,12], showing the predicted increases in the regions of the plasmons and the decrease at low energy. However, from a quantitative point of view, the semiclassical theory predicts a universal energy-dependent enhancement factor, the ratio of the cross sections of confined and free atoms, while our *ab initio* calculations show that this factor differs widely (by an order of magnitude or so) for different atoms, using the examples of Mg $3s$ and Ar $3p$.

ACKNOWLEDGMENTS

This work was supported by NSF and DOE, Basic Energy Sciences.

[1] L. Moro, R. S. Rouff, C. H. Becker, V. C. Lorents, and R. Malhotra, J. Chem. Phys. **97**, 6801 (1993).
[2] A. Gromov, E. Krätshmer, N. Krawez, R. Tellgmann, and E. B. Campbell, Chem. Commun. (Cambridge) **20**, 2003 (1997).
[3] B. Sundqvist, Adv. Phys. **48**, 1 (1999), and references therein.
[4] L. Dunsch and S. Yang, Electrochem. Soc. Interface **15**, 34 (2006).
[5] V. K. Dolmatov, A. S. Baltenkov, J.-P. Connerade, and S. T. Manson, Radiat. Phys. Chem. **70**, 417 (2004).
[6] C. Ju, D. Suter, and J. Du, Phys. Rev. A **75**, 012318 (2007).
[7] W. Harneit, Phys. Rev. A **65**, 032322 (2002).
[8] B. E. Kane, Nature (London) **393**, 133 (1998).
[9] A. Takeda, Y. Yokoyama, S. Ito, T. Miyazaki, H. Shimotani, K. Yakigaya, T. Kakiuchi, H. Sawa, H. Takagi, K. Kitazawa, and N. Dragoe, Chem. Commun. (Cambridge) **8**, 912 (2006).
[10] L. Becker, R. J. Poreda, and T. E. Bunch, Proc. Natl. Acad. Sci. U.S.A. **97**, 2979 (2000).
[11] J.-P. Connerade and A. V. Solov'yov, J. Phys. B **38**, 807 (2005).
[12] S. Lo, A. V. Korol, and A. V. Solov'yov, J. Phys. B **40**, 3973 (2007) (private communication).
[13] M. E. Madjet, H. S. Chakraborty, and S. T. Manson, Phys. Rev. Lett. **99**, 243003 (2007).
[14] E. Broclawik and A. Eilmes, J. Chem. Phys. **108**, 3498 (1998).
[15] A. Rüdel, R. Hentges, U. Becker, H. S. Chakraborty, M. E. Madjet, and J. M. Rost, Phys. Rev. Lett. **89**, 125503 (2002).
[16] M. J. Puska and R. M. Nieminen, Phys. Rev. A **47**, 1181 (1993).
[17] S. W. J. Scully, E. D. Emmons, M. F. Gharaibeh, R. A. Phaneuf, A. L. D. Kilcoyne, A. S. Schlachter, S. Schippers, A. Müller, H. S. Chakraborty, M. E. Madjet, and J. M. Rost, Phys. Rev. Lett. **94**, 065503 (2005).
[18] S. W. J. Scully, E. D. Emmons, M. F. Gharaibeh, R. A. Phaneuf, A. L. D. Kilcoyne, A. S. Schlachter, S. Schippers, A. Müller, H. S. Chakraborty, M. E. Madjet, and J. M. Rost, Phys. Rev. Lett. **98**, 179602 (2007).
[19] M. E. Madjet, H. S. Chakraborty, and J. M. Rost, J. Phys. B **34**, L345 (2001).
[20] P.-A. Hervieux, M. E. Madjet, and H. Benali, Phys. Rev. A **65**, 023202 (2002).
[21] W. Ekardt, Phys. Rev. B **31**, 6360 (1985).
[22] M. E. Madjet, H. S. Chakraborty, J. M. Rost, and S. T. Manson, J. Phys. B **41**, 105101 (2008).
[23] M. Stener, G. Fronzoni, D. Toffoli, P. Colavita, S. Furlan, and P. Decleva, J. Phys. B **35**, 1421 (2002).
[24] H. A. Bethe and E. E. Salpeter, *Quantum Mechanics of One- and Two-Electron Atoms* (Springer-Verlag, Berlin, 1958), p. 255.
[25] J.-P. Connerade, V. K. Dolmatov, and S. T. Manson, J. Phys. B **33**, 2279 (2000).
[26] A. F. Starace, in *Handbuch der Physik*, edited by W. Mehlhorn (Springer, Berlin, 1982), Vol. 31, pp. 1–121.